A Novel Method for Porosity Measurement of Various Surface Layers of Nanofibers Mat Using Image Analysis for Tissue Engineering Applications

L. Ghasemi-Mobarakeh, D. Semnani, M. Morshed

Department of Textile, Isfahan University of Technology, Isfahan, Iran

Received 18 November 2006; accepted 1 June 2007
DOI 10.1002/app.26949
Published online 29 July 2007 in Wiley InterScience (www.interscience.wiley.com).

ABSTRACT: Research in polymer nanofibers has undergone significant progress in the last decade. One of the main driving force for this progress is the increasing use of these polymer nanofibers for tissue engineering. Adequate porosity and surface area are widely recognized as important parameters in the design of scaffolds for tissue engineering and therefore measurement of porosity is very important. Previous methods such as mercury measurement, indirect method, the porosity measurement based on density of nanofibers do not measure the porosity of various surface layers. The goal of this study is measurement of porosity of various surface layers of scaffold. Image analysis was used for this purpose. SEM images of nanofibers mat were converted to binary images using different thresholds and porosity of scaffold was measured in various layers. On the basis of the results of our study, this method can be applied to porosity measurement of various surface layers of nanofibers mat. The results showed that porosity of various surface layers is related to the number of layers of nanofibers mat. © 2007 Wiley Periodicals, Inc. J Appl Polym Sci 106: 2536–2542, 2007

Key words: tissue engineering; scaffold; porosity; image analysis; nanotechnology; fibers

INTRODUCTION

Polymer nanofibers mat, an important class of nanomaterials, have attracted much interest in the last 10 years.[1] Polymeric nanofibers can be produced by a number of techniques such as drawing, template synthesis, phase separation, self-assembly, and electrospinning.[2–4]

Electrospinning is a well-established process capable of producing ultrafine fibers by electrically charging a suspended droplet of polymer melt or solution. A high voltage power supply is required to create an electrically charged jet of polymer solution or melt.[3] An attractive feature of electrospinning is the simplicity and inexpensive nature of setup.[5] Electrospinning has the following advantages: it can produce continuous fibers; it can be applied to a wide range of polymers; the thickness of mat can be controlled by adjusting the collection time during the electrospinning; the dimensions and surface morphologies of the electrospun fibers can be varied by altering the solution properties and processing parameters.[6] Small fiber diameter and porous structure of the nanofibers mat give rise to a large specific surface area. This is advantageous in a wide variety of applications such as high performance filters, scaffold in tissue engineering, separation membranes, reinforcement in composite materials, templates for the preparation of functional nanotubes, and many others.[7] Much interest has been generated recently in the area of tissue engineering.[8] Tissue engineering has been defined as an interdisciplinary field that applies the principles of engineering and the life science toward the development of biological substitutes that restore, maintain or improve tissue function.[2] There are generally three key aspects to consider in any tissue-engineered construction: the cells, the scaffold or biomaterial construct, and the cell–material interaction.[2,9] There are a few basic requirements that have been widely accepted for scaffolds. A scaffold has to have high porosity and proper pore size to permit the ingress of cells and nutrients.[2,10–12] Adequate porosity and surface area are widely recognized as important parameters in the design of scaffolds for tissue engineering.[13] A large pore volume is required to accommodate and subsequently deliver a cell mass sufficient for tissue repair.[10] The pores of scaffolds are very important for cell growth. The cells adhere to the surface of the scaffolds, absorb nutrient, and remove metabolite through the pore.[14] The diameter of cells in suspension dictates the minimum pore size, which varies from one cell type to another and must be controlled carefully.[10,15] If the pores are too small the cells cannot enter and if they are too large the cells cannot adhere.[14] The scaffold should provide an open porous network for uni-

Correspondence to: M. Morshed (morshed@cc.iut.ac.ir).

Journal of Applied Polymer Science, Vol. 106, 2536–2542 (2007)

form cell distribution during seeding and for mass transport of soluble signaling molecules, nutrients and metabolic waste removal.[16] Pores in the scaffold make-up the space in which cells reside. Pore properties such as porosity, dimension, and volume are parameters directly related to the success of a scaffold. High porosity provides more structural space for cell accommodation.[12] Another important consideration is the continuity of the pores within a synthetic matrix. Material transport and cell migration will be inhibited if the pores are not interconnected.[10]

There are several methods that can be used to estimate the porosity such as sorption and mercury porosimetery.[17] The sorption method determines the amount of vapors of the low-molecular weight liquid that are absorbed by a body at different vapor pressures and plots the isotherms of sorption and desorption with the subsequent calculation.[16,17]

The most common methodology adopted for membrane pore characterization is mercury porosimetry. The theory of all mercury porosimeters is based on physical principle that a nonreactive nonwetting liquid will not penetrate pores until sufficient pressure is applied to force its entrance.[4,17] The advantage of using a mercury porosimeter is that in addition to the pore size and its distribution, the total pore volume and the total pore area can also be determined.[4] A major drawback of using mercury is that generally very high pressures are required as the pore size diminishes. Therefore, when thin sections are analyzed, there is a high possibility that membrane can be destroyed at higher pressures. This is especially true for electrospun nanofibrous membranes because the pores in electrospun membrane are not rigid enough. The other drawbacks of using mercury are its cost and toxicity.[4] Other methods also have been used for determination of scaffold porosity. Yang and Ramakrishna reported an indirect method for porosity measurement of nanostructured PLLA scaffold that was prepared by phase separation method.[18] In this method considering the wetting properties of PLLA nanofibrous scaffold, water was selected as a nonwetting agent, since it would not penetrate into the pores and ethanol as a wetting agent, since it can penetrate into the scaffold to measure the porosity of PLLA scaffold.[18] According to the results obtained by this method, the porosity of scaffold has been reported between 81.5% and 93.2% depending on the fiber diameter.[18] Eugene and Todd by applying density measurement determined the porosity of electrospun scaffolds.[19]

The results obtained by this method showed the porosity to be higher than 80% for nanofiber scaffold.[19] On the other hand, Wei and Zuwei calculated the porosity of nanofibers scaffold using the following equation[20]:

$$\text{Porosity} = \left(1 - \frac{\text{Nanofiber mat apparant density}}{\text{Bulk density of scaffold}}\right) \times 100$$

$$\text{Nanofiber apparent density} = \frac{\text{Nanofiber mat mass}}{\text{Nanofiber mat thickness} \times \text{Nanofiber mat area}}$$

The thickness of nanofibers mat was measured by a micrometer. According to this method, the porosity of nanofibers mat was reported to be around 60–70%.[20]

The goal of this study is porosity measurement of various surface layers of nanofibers mat, which are visible in SEM image. The other methods of porosity determination cannot be used for porosity measurement of various surface layers and can only measure the total porosity of nanofiber mat. The investigation of the porosity measurement of various surface layers is very interesting in tissue engineering application.

MATERIALS AND METHODS

Materials

Poly(ε-caprolactone) (PCL) with number–average molecule weight (M_n) of 80,000 was purchased from

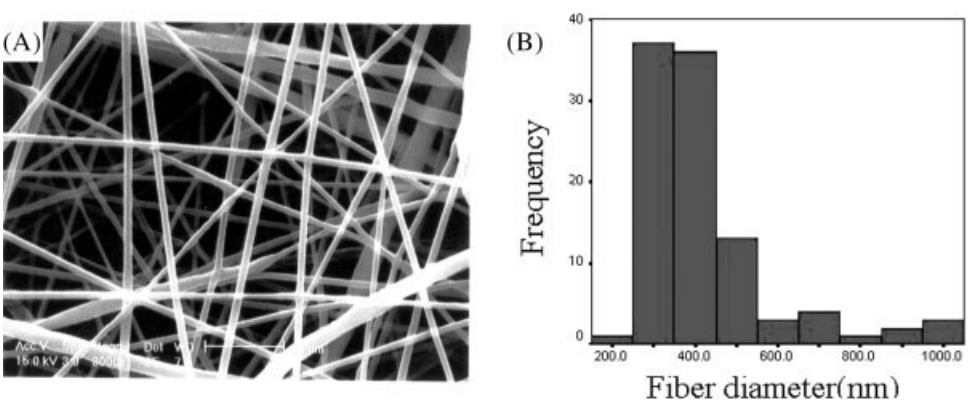

Figure 1 SEM image: (A) as-spun PCL nanofibers, (B) fiber diameter distribution.

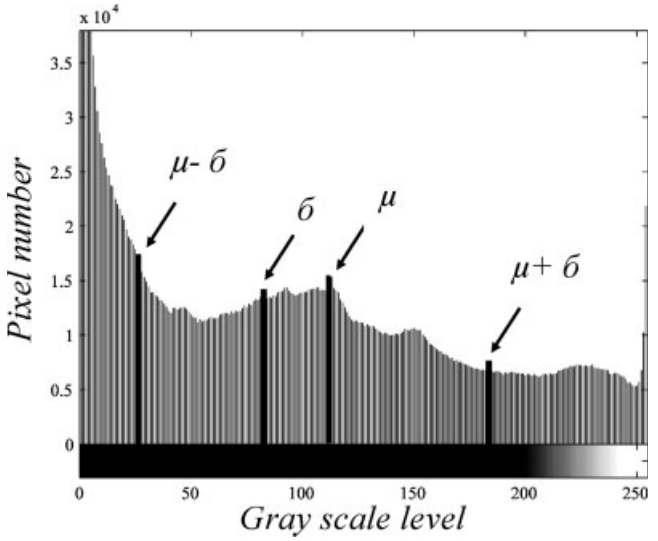

Figure 2 Image histogram of Figure 1(A).

Aldrich (Sigma-Aldrich, St. Louis, MO). Methylene chloride (MC), DMF, and NaOH were purchased from Merck (Germany).

The polymer solution with concentration of 10 wt % was prepared by dissolving PCL in a mixture of MC/DMF solvents with the ratio of 80/20 and was stirred for 24 h at room temperature. The solution was electrospun from a 10-mL syringe with a needle diameter of 0.6 mm. Upon applying a high voltage (12 kV), a fluid jet was ejected from the tip of the needle. As the jet accelerated toward a target, which was placed 20 cm from the syringe tip, the solvent evaporated and polymer nanofibers were collected on an aluminum foil. The polymer solutions were delivered via a syringe pump to control the mass flow rate. The mass flow rate of the solutions was 4 mL/h. All electrospinnings were carried out at room temperature.

Morphology of 10 electrospun PCL nonwoven mats was studied by scanning electron microscopy (SEM) after gold coating with magnification of 3000 and 6000. Figure 1(A) shows a SEM micrograph of the as electrospun PCL nanofibers. As shown in Figure 1(B), average fiber diameter was found to be 418 nm with a range of 225–1000 nm.

Methodology

The SEM photographs of nanofibers mat were scanned using a scanner (hp scanjet 3670). The resolution of scanned images was 600 dpi and gray scale level of 256. This resolution of scanning was found by experimental observations. Lower resolution makes the analysis poor while higher resolution dose not improve the analysis results and causes reduction in analysis speed.

After inserting the obtained images of SEM pictures to the computer as BMP format of 256 gray scale, a novel image analysis technique was prepared to determine the porosity of various layers of nanofibers mat

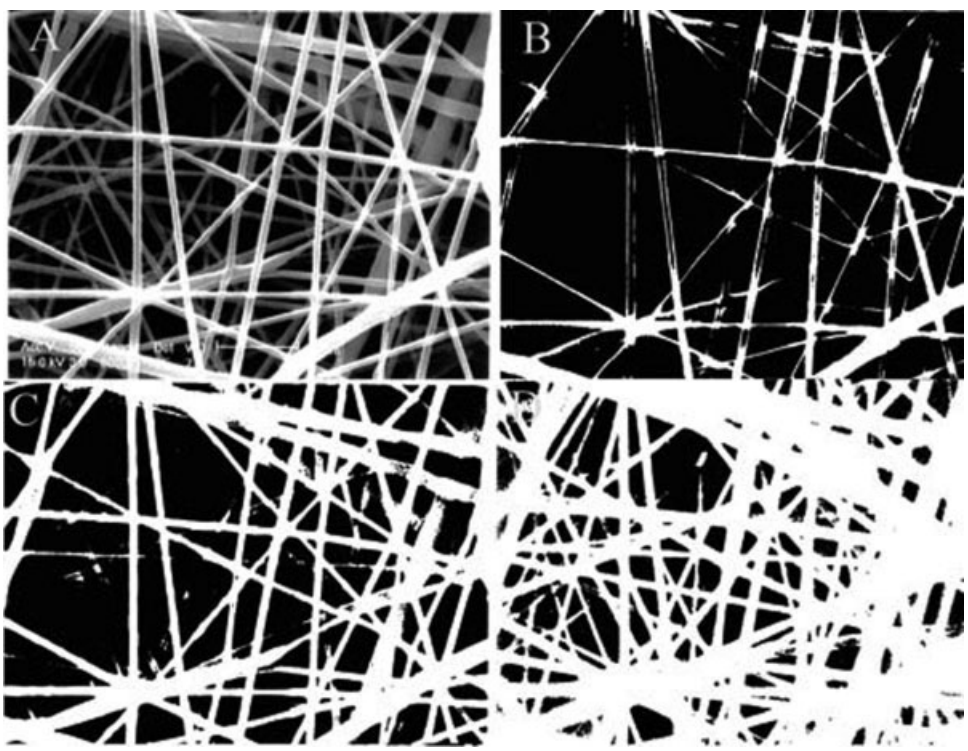

Figure 3 Various binary images with different thresholds: (A) original image, (B) binary image with threshold of the (μ + б)/255, (C) binary image with threshold of the μ/255, (D) binary image with threshold of the (μ − б)/255.

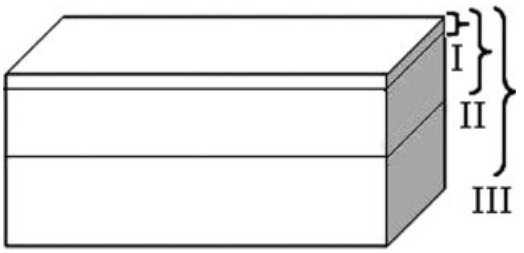

Figure 4 Schematic representation of various layers of nanofibers mat with different threshold: (I) the layers that can be seen by applying threshold 1, (II) the layers that can be seen by applying threshold 2, and (III) the layers that can be seen by applying threshold 3.

samples. The gray scale image was converted to binary form by calculating the threshold. It was found in this study that by changing the threshold, various layers of nanofibers mat could be seen.

The mean and standard deviation of image histogram have been applied by Semnani to specify different parts of the knitted fabric structure.[21] This method of image analysis depends on the gray scale level processing based on image structure.[21]

It was observed that the reflection of upper layers of fibers is more than the lower layers. Therefore, in SEM images of nanofibers mat, the intensity of pixels in upper fibers layers in comparison to lower layers of fibers is higher. Consequently, it is possible to analyze the SEM images of nanofibers mat by using gray scale level processing where the upper and lower layers could be identified on the basis of their intensity region and from calculating the appropriate threshold.

After many experiments, three thresholds were found for converting the original image to binary form based on mean and standard deviation of image pixel values. These thresholds were found as follows:

1. Threshold 1: $(\mu + б)/255$
2. Threshold 2: $\mu/255$
3. Threshold 3: $(\mu - б)/255$

where μ and $б$ are the mean and standard deviation of the image matrix, respectively. By using these thresholds, we can classify various layers of nanofibers mat. The first threshold eliminates lower layers and only the surface layers are obtained, the second threshold can represent sum of surface and middle layers, and third threshold shows all of the visible layers. Figure 2 shows the configuration of histogram related to Figure 1(A).

Figure 3 shows the various binary images of the Figure 1(A) with different thresholds.

Figure 4 represents schematically various layers of nanofibers mat that has been classified by different thresholds. Region I presents surface layers. By applying threshold 1, only surface layers can be seen in binary image [Fig. 3(B)]. Threshold 2 consider the sum of surface to middle layers [Fig. 3(C)], shown as Region II in Figure 4. Total visible layers can be seen by applying threshold 3, shown as Region III in Figure 4.

TABLE I
Porosity Measurement of Various Binary Images of Figure 1(A) with Various Thresholds

P_1	P_2	P_3
80.1010	54.8440	20.0173

After converting the original image to various binary images, the porosity in each binary image can be calculated using the mean intensity of images as follows:

$$P = \left(1 - \frac{n}{N}\right) \times 100$$

where n is the number of white pixels, N is the total number of pixels in binary image, and P is the porosity percentage of binary image. The porosity percentage of binary images with thresholds of 1, 2, and 3 will be presented as P_1, P_2, and P_3, respectively in next sections of this article.

RESULTS AND DISCUSSION

The results of porosity calculation of various binary images of the Figure 1(A) with various thresholds are shown in Table I.

As can be seen in Figure 3, when $(\mu + б)/255$ was selected as threshold, only the surface layers (i.e., Region I) of the nanofibers mat can be seen. By selecting $\mu/255$ as threshold, the middle layers (i.e., Region II) and by choosing $(\mu - б)/255$ as threshold, all of the visible layers (i.e., Region III) of nanofibers mat can be seen. As can be seen in Figure 3, when there are more layers, the fibers overlap with each other and therefore the obtained porosity in this case is less than the one with less layers of fibers and this could

TABLE II
Porosity Measurement of Various Binary Images of Different Samples with Various Thresholds

Sample	Magnification	P_1	P_2	P_3
1	3000	86.6224	53.7919	15.0197
2	3000	80.5995	54.4068	22.3248
3	3000	77.0187	56.7961	16.7212
4	3000	81.26665	54.1022	20.5998
5	6000	71.4993	53.2412	26.4688
6	6000	80.0607	54.8979	19.7359
7	6000	74.0644	57.9342	19.6167
8	6000	77.4874	55.3328	12.5067
9	6000	78.5912	56.1179	16.2035

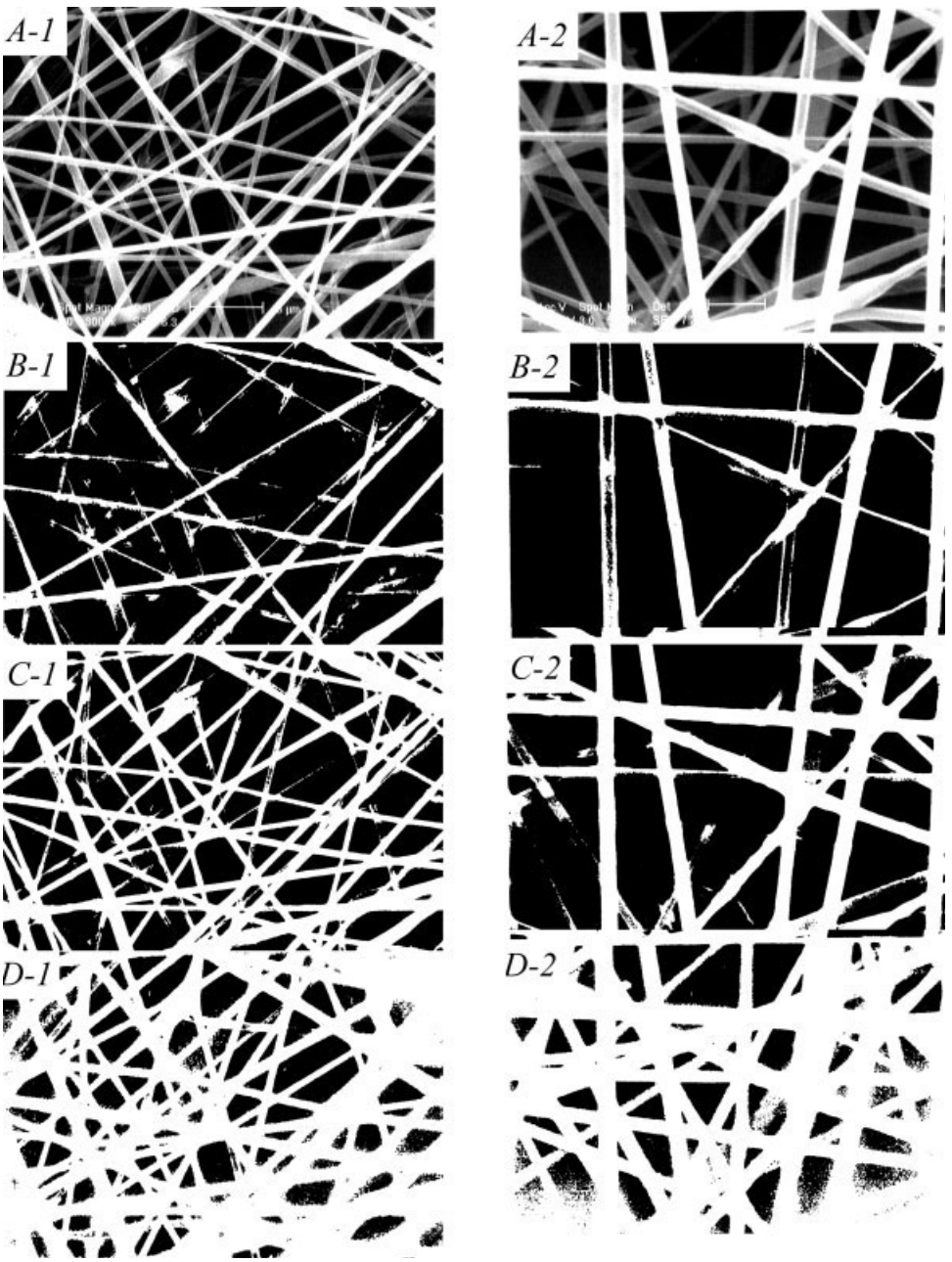

Figure 5 Various binary images with different thresholds: (A) original image, (B) binary image with threshold of the (μ + б)/255, (C) binary image with threshold of (μ/255), (D) binary image with threshold of the (μ − б)/255; the numbers 1 and 2 show sample numbers; magnification of the Sample 1: 3000; magnification of the Sample 2: 6000.

lead to higher percentage of porosity obtained for surface layers. The results in Table I confirm this finding.

To study the consistency of this method, it was also applied to other samples with magnifications of the 3000 and 6000 to determine the porosity of various layers. The porosity values of various binary images of different samples are shown in Table II.

As can be seen from this table the porosity of the surface layers (Region I) is more than the porosity of the middle layers (Region II) and the porosity of middle layers is more than the porosity of total surface layers (Region III). These results confirm those shown in Table I. Consequently, it can be concluded that the porosity measurement based on image analysis that is reported in this study can measure the porosity of various layers of nanofibers. In other words, the difference between the porosity of the various surface layers can be found.

The results in Table II show that the porosity of the Region III in comparison to the porosity of Regions II and I is low (15–20%). This is because more fibers overlap with each other. Our results show that porosity is related to the number of layers and it approaches

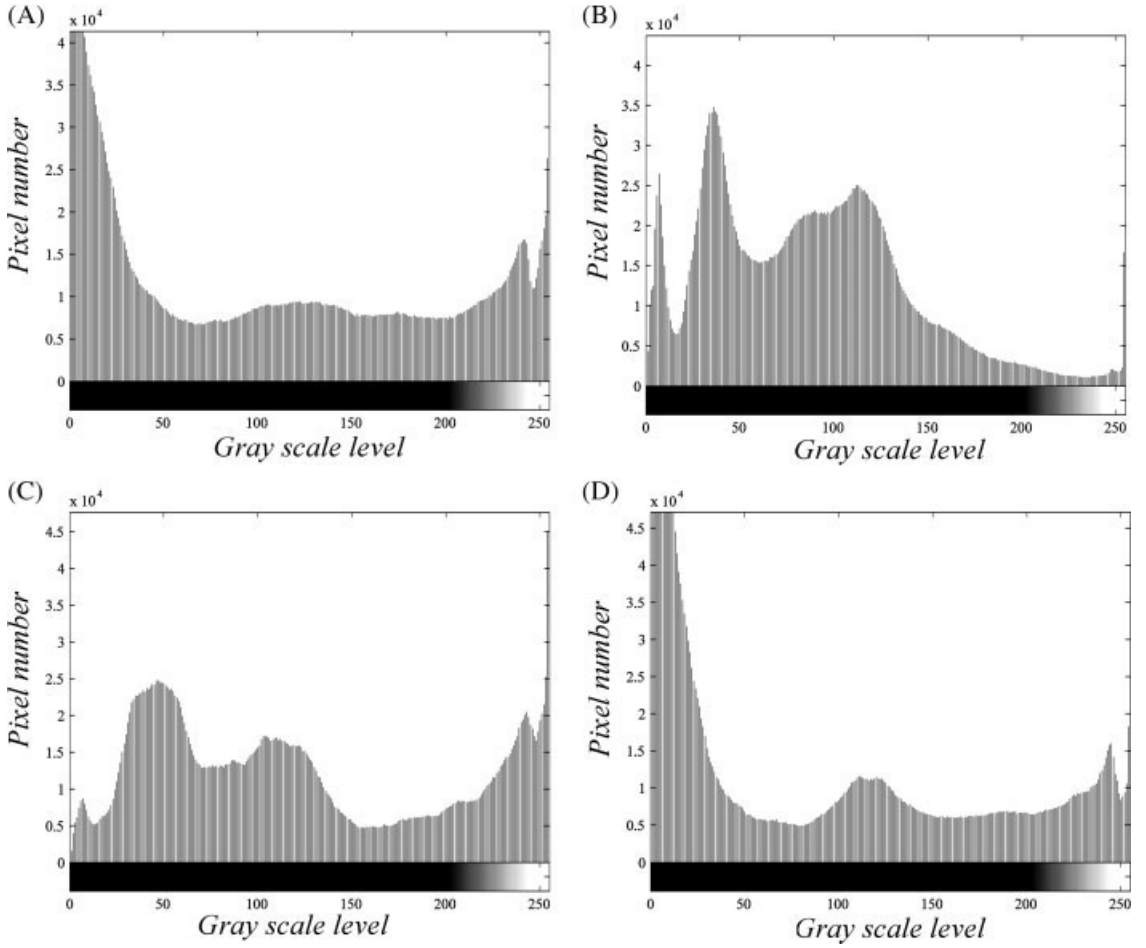

Figure 6 Histogram of different samples. Magnification of (A) and (B): 3000 and magnification of (C) and (D): 6000.

a minimum value by increasing the number of layers due to more overlapping of fibers with each other when more layers are present.

Figure 5 shows various binary images with different thresholds for various samples with magnification of 3000 and 6000.

Figure 6 shows the histogram of various images with different magnification.

As can be seen in Figures 5 and 6, the results are not dependent upon the magnification or histogram of images. Therefore, this method let one to calculate porosity of various layers in most image magnifications and most image histograms. It should be pointed out that the choice of suitable magnification is related to fiber diameter and where experiments show, magnifications of more than 2000 is suitable for fibers with 480 nm diameter. Therefore, fiber diameters obtained by SEM images should be more than 1 mm (48 pixels for image with resolution of 1200). Also the SEM images should have optimum resolution, clarity, and brightness.

The results obtained by mercury porosimetry analysis has demonstrated the porosity of more than 80% for nanofibers mat.[6,22,23] The results of indirect method measurements have shown the porosity value of more than 90% for nanostructured porous PLLA scaffold.[18] The results obtained by density measurement have shown the porosity values of higher than 80% for nanofiber scaffolds.[19] While the porosity measurements based on thickness and apparent density of nanofibers mat that was reported by Wei and Zuwei[20] demonstrated the porosity of between 60 and 70%. The aforementioned other methods cannot measure the porosity of various layers and measure the total porosity of nanofiber mat.

It appears that by using mercury porosimetry method, which is a common technique for porosity measurement, very reliable results cannot be obtained for nanofibers mat. This could be due to high pressure that is applied in this method. Besides, the structure of nanofibers mat is not rigid and strong enough to stand intact to such a high pressure. Therefore, due to high pressure the pores can get enlarged. This could lead to overestimation of porosity values.

In many applications of nanofibers mat such as filters and scaffolds for tissue engineering, it is very important to know the porosity of various layers. For example, in scaffolds, the highly porous fibrous mate-

rials not only have high specific surface area but also provide a structure inductive for tissue engineering. Understanding the dynamic effects of 3-D matrix structure and its pore size on cell organization, proliferation, differentiation, and function is very important and is the first step that leads to the optimal design of scaffolds for tissue engineering. Previous works did not specifically report the porosity of various surface layers of scaffold, but the advantage of this method is porosity measurement of various surface layers of nanofibers mat.

CONCLUSION

With the aid of image analysis, the present study explored the possibility of porosity measurement of various surface layers of nanofibers mat. The results of this investigation reveal that image analysis can easily be applied for porosity measurement of various layers. The results showed that this method is not dependent on the magnification and histogram of images. The measurement by such a simple method can be applied in a variety of applications such as filters and scaffolds for tissue engineering that the measurements of porosity in various layers are very important. The porosity measurements based on other methods such as mercury porosimetry and indirect method and calculation of porosity by density measurement all show high porosity values (higher than 80%) for the nanofibers mat and cannot be used for porosity measurement of various surface layers of nanofibers mat. Current work is in progress to determine the shape, size, and other parameters of pores based on image analysis.

References

1. Yanzhong, Z.; Seeram, R. J Mater Sci Mater Med 2005, 15, 933.
2. Peter, X. M. Materials Today, May 2004, pp 30–40.
3. Smith, L. A. Colloids Surf B Biointerf 2004, 39, 125.
4. Ramakrishna, S.; Fujihara, K. An Introduction to Electrospinning and Nanofibers; World Scientific Publishing: Singapore, 2005; pp 199–206.
5. Quynh, P. P.; Upma, S. Tissue Eng 2006, 12, 1197.
6. Yang, F.; Kotaki, M. J Biomater Sci Polym Ed 2004, 15, 1483.
7. Huang, Z. M.; Zhang, Y. Z. Compos Sci Technol 2003, 63, 2223.
8. Khil, M. S.; Shanta, R. B. J Biomed Mater Res 2005, 72B, 117.
9. Ramalingam, M.; Seeram, R. Tissue Eng 2006, 12, 435.
10. Shoufeng, Y.; Zhaohui, D. U. Tissue Eng 2001, 7, 679.
11. Zuwei, M. A.; Masaya, K. Tissue Eng 2005, 11, 101.
12. Shobana, S. A. M. Sc. Thesis (Biomedical Engineering), New Jersey Institute of Technology, January 2004.
13. Manuela, E. G.; Heidi, L. H. Tissue Eng 2006, 12, 801.
14. Guixin, S.; Qing, C. Polym Adv Technol 2002, 13, 227.
15. Buckley, C. T. In Topics in Bio-Mechanical Engineering; Prendergast, P. J., McHugh, P. E., Eds.; Trinity Centre for Bioengineering and the National Centre for Biomedical Engineering Science: Dublin and Galway, 2004; pp 147–166.
16. Victor, J. C.; Peter, X. M. Biomaterials 2004, 25, 2065.
17. Tager, A. Physical Chemistry of Polymers; Mir Publishers: Moscow, 1978; pp 593–600.
18. Yang, F.; Ramakrishna, S. Biomaterials 2004, 25, 1891.
19. Eugene, D.; Todd, A. J Biomed Mater Res 2004, 71B, 144.
20. Wei, H.; Zuwei, M. Biomaterials 2005, 26, 7606.
21. Semnani, D.; Lattifi, M. J Text Inst 2005, 96, 295.
22. Kyong, S. R.; Lim, J. Biomaterials 2006, 27, 1452.
23. Shanta, R.; Narayan, B. Biomaterials 2004, 25, 2595.